Electronic Supplementary Material (ESI) for Nanoscale.

Supporting Information

Metal-organic framework derived amorphous VOx coated Fe3O4/C hierarchical nanospindle as anode material for superior lithium-ion batteries

Bowen Cong, Yongyuan Hu, Shanfu Sun, Yu Wang *, Bo Wang, Huabin Kong, Gang Chen *

MIIT Key Laboratory of Critical Materials Technology for New Energy Conversion and Storage, School of Chemistry and Chemical Engineering, Harbin Institute of Technology, Harbin 150001, P. R. China

The supporting information includes 13 figures, 2 tables, and 17 references.

* Corresponding author:

Email: wangyu1012@hit.edu.cn (Yu Wang);

Email: gchen@hit.edu.cn (Gang Chen);

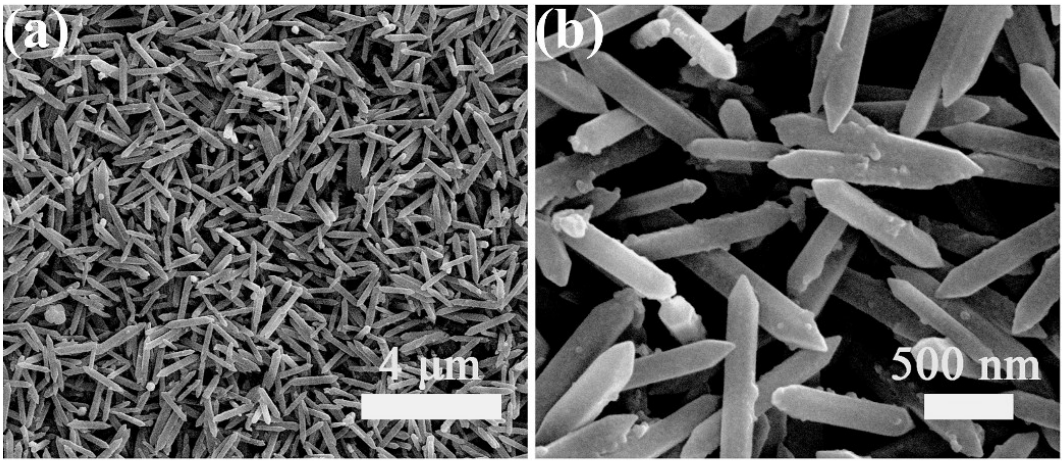

Fig. S1 SEM images of Fe-MOF nanospindles at (a) low- and (b) high-magnification.

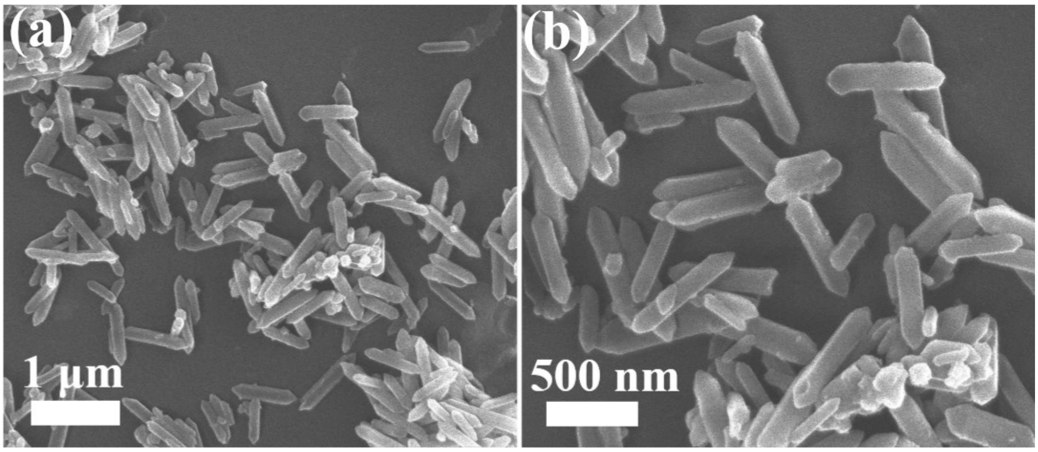

Fig. S2 SEM images of Fe-MOF@V_2O_5 nanospindles at (a) low- and (b) high-magnification.

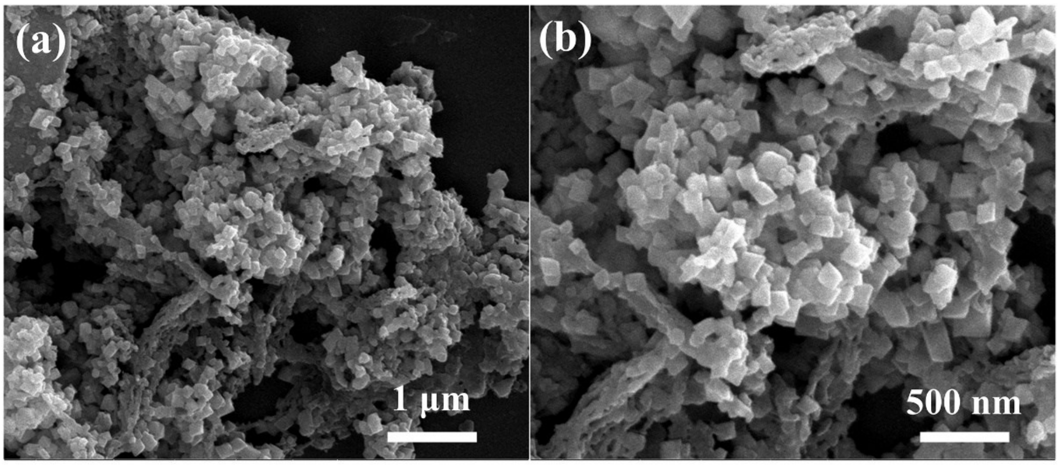

Fig. S3 SEM images of the Fe_3O_4/C sample at (a) low- and (b) high-magnification.

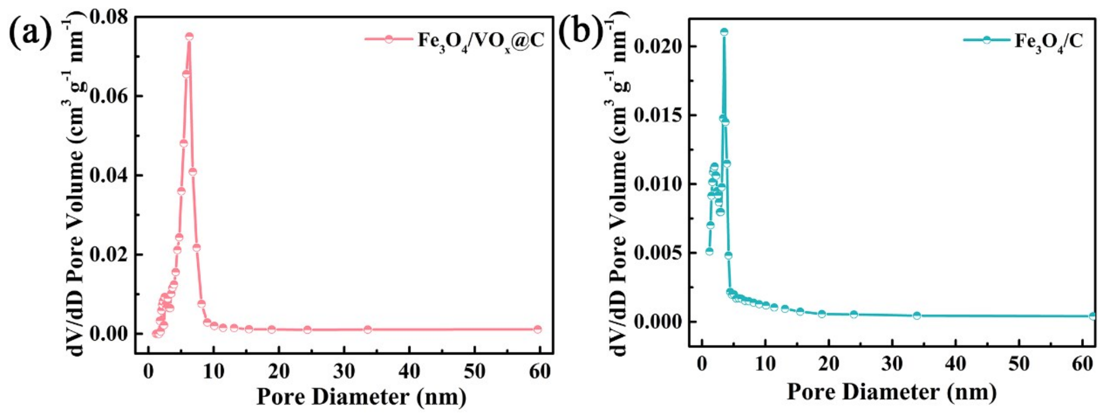

Fig. S4 The pore size distribution of (a) $Fe_3O_4/C@VO_x$ and (b) Fe_3O_4/C samples.

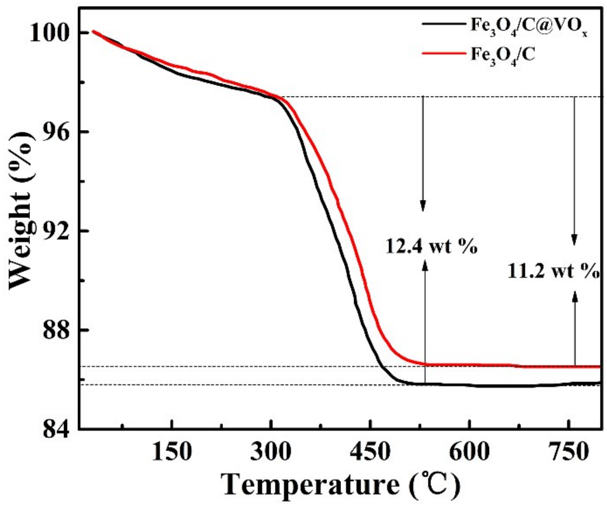

Fig. S5 Thermo gravimetric analysis (TGA) curves of $Fe_3O_4/C@VO_x$ and Fe_3O_4/C samples at a temperature ramp of 10 ℃ min^{-1} in air.

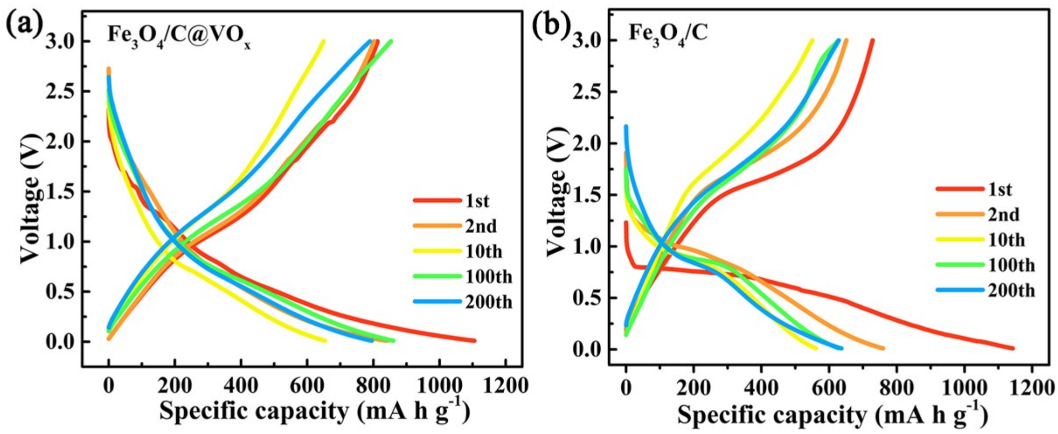

Fig. S6 Charge-discharge curves of (a) $Fe_3O_4/VO_x@C$ and (b) Fe_3O_4/C at the current density of 1000 mA g^{-1}.

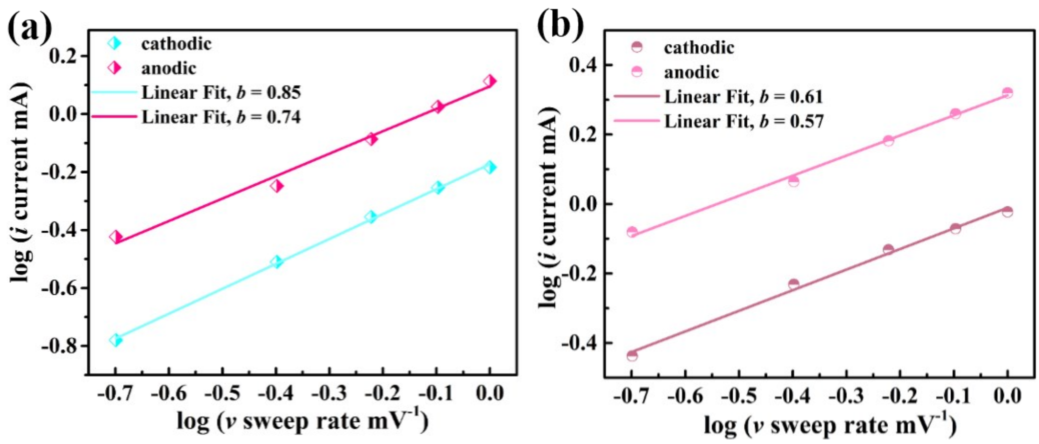

Fig. S7 *b*-values evaluation of (a) Fe_3O_4/C@VO_x and (b) Fe_3O_4/C using the relationship between peak current and scan rate.

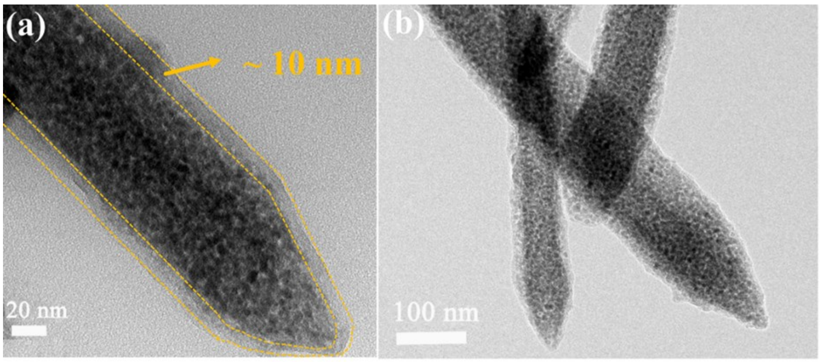

Fig. S8 TEM images of Fe_3O_4/C@VO_x-1 (the thickness of the VO_x layer is ~ 10 nm) at (a) high- and (b) low- magnification.

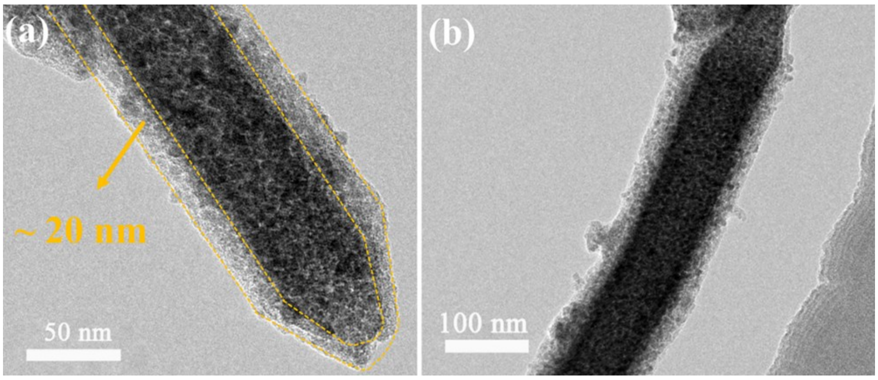

Fig. S9 TEM images of Fe_3O_4/C@VO_x-2 (the thickness of the VO_x layer is ~ 20 nm) at (a) high- and (b) low- magnification.

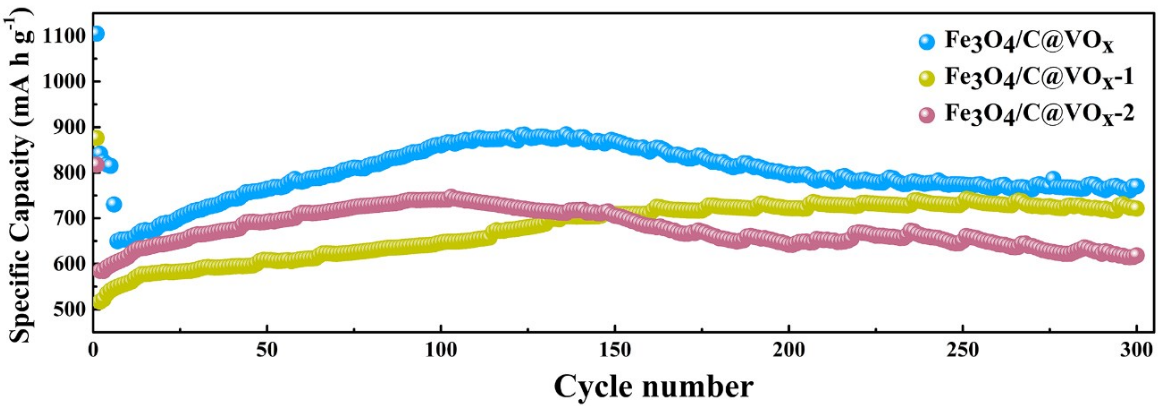

Fig. S10 Charge/discharge capacities of Fe_3O_4/C@VO_x sample with different thickness of the VO_x layer is ~ 5 nm (Fe_3O_4/C@VO_x), ~ 10 nm (Fe_3O_4/C@VO_x-1) and ~ 20 nm (Fe_3O_4/C@VO_x-2), respectively.

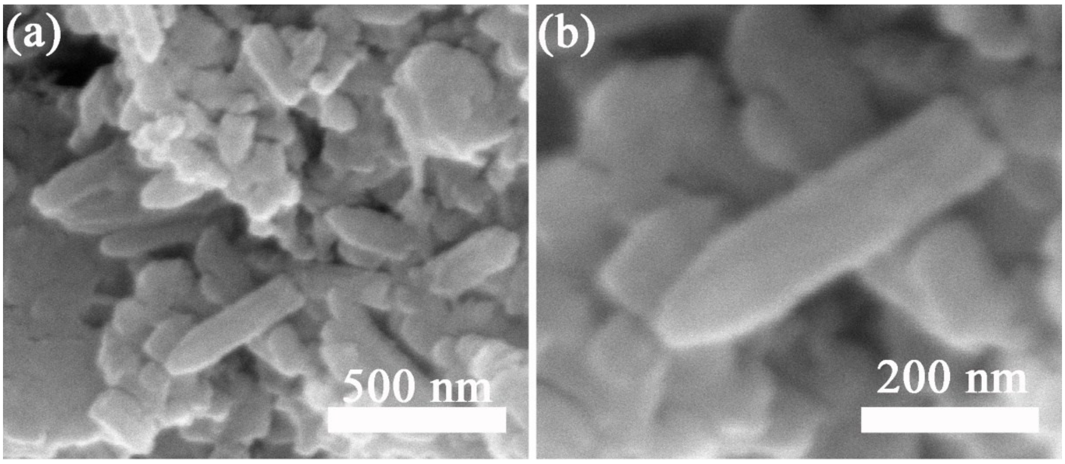

Fig. S11 SEM images of the Fe_3O_4/C@VO_x electrode after 500 cycles at 1 A g^{-1} current density in (a) low- and (b) high-magnification.

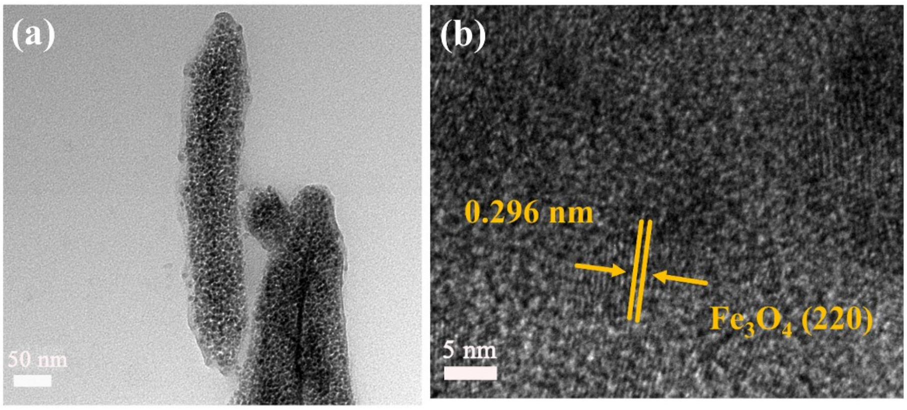

Fig. S12 The Fe_3O_4/C@VO_x electrode after 500 cycles at 1000 mA g^{-1} current density in (a) TEM and (b) HRTEM images.

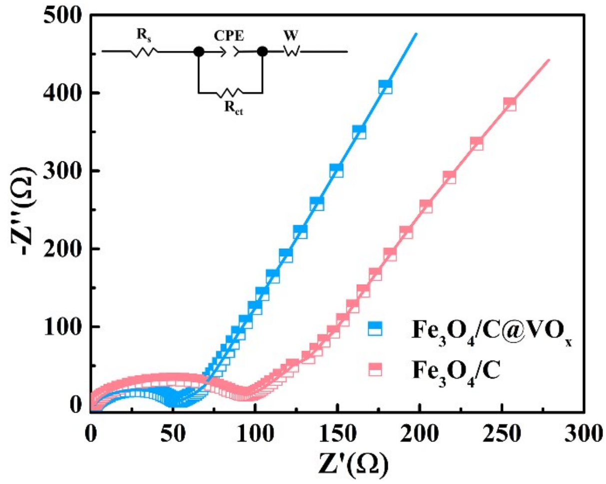

Fig. S13 Nyquist plots of fresh cells (inset: equivalent circuit for plot fitting).

Table S1 Comparison of the LIBs performance of $Fe_3O_4/C@VO_x$ electrode material and recently reported Fe_3O_4 and Fe_3O_4/C based materials in the literature

Electrode material	Current density (mA g^{-1})	Reversible capacity (mA h g^{-1})	Cycle number (Times)	Ref.
Hollow Fe_3O_4/C spheres	200	984	70	[1]
Yolk–Shell $Fe_3O_4@C$ Composite	1000	750	70	[2]
$FeO_x@C$ yolk-shelled structure	200	790	100	[3]
Graphene-Encapsulated Fe_3O_4 nanoparticles	100	650	100	[4]
Carbon-coated Fe_3O_4 nanospindles	500	530	80	[5]
Fe_3O_4/C nanotubes	150	600	100	[6]
Fe_3O_4/C microrods	200	650	100	[7]
Porous Fe_3O_4/C Microbelts	100	710	50	[8]
3D Hierarchical Fe_3O_4/Graphene Composites	92.5	609	50	[9]
Mesoporous $Fe_3O_4@C$ Microcapsules	100	928	50	[10]
Fe_3O_4/rGO nanorod	500	890	100	[11]
Fe_3O_4/C Filament Network	100	1278	100	[12]
Hierarchical 3D Fe_3O_4@porous carbon matrix/graphene	200	1077	100	[13]
$Fe_3O_4@C$ yolk-shell nanorods	500	954	200	[14]
$Fe_3O_4@C$ nanosheet	200	1232	120	[15]
Fe_3O_4/C nanofibers	500	761	300	[16]
Fe_3O_4 microflowers	100	1000	50	[17]
$Fe_3O_4/C@VO_x$ nanospindles	**200**	**1336**	**300**	**Our work**

Table S2 Electrochemical Impedance Parameters of the $Fe_3O_4/C@VO_x$ and Fe_3O_4/C

Samples	$R_s(\Omega)$	$R_{ct}(\Omega)$
$Fe_3O_4/C@VO_x$	1.96	49.85
Fe_3O_4/C	2.41	91.50

References

1 Q. M. Zhang, Z. C. Shi, Y. F. De, J. Zheng, G. C. Liu, and G. H. Chen, *J. Power Sources*, 2012, **197**, 305-309.

2 Y. Zhao, J. X. Li, C. X. Wu, Y. H. Ding and L. H. Guan, *ChemPlusChem*, 2012, **77**, 748-751.

3 H. W. Zhang, L. Zhou, O. Noonan, J. Martin, K. Whittaker and C. Z. Yu, *Adv. Funct. Mater.*, 2014, **24**, 4337–4342.

4 J. Z. Wang, C. Zhong, D. Wexler, N. H. Idris, Z. X. Wang, L. Q. Chen and H. K. Liu, *Chem. Eur. J.* 2011, **17**, 661 – 667.

5 W. M. Zhang, X. L. Wu, J. S. Hu, Y. G. Guo and L. J. Wan, *Adv. Funct. Mater.*, 2008, **18**, 3941–3946.

6 H. Luo, K. Huang, B. Sun and J. X. Zhong, *Electrochim. Acta*, 2014, **149**, 11-17.

7 Y. R. Wang, L. Zhang, X. H. Gao, L. Y. Mao, Y. Hu and X. W. Lou, *Small* 2014, **14**, 2815–2819.

8 L. M. Lang and Z. Xu, *ACS Appl. Mater. Inter.*, 2013, **5**, 1698−1703.

9 X. Y. Li, X. L. Huang, D. P. Liu, X. Wang, S. Y, Song, L. Zhou and H. J. Zhang, *J. Phys. Chem. C*, 2011, **115**, 21567–21573.

10 S. M. Yuan, J. X. Li, T. Tang, L. W. Su, L. Liu and Z. Zhou, *ACS Appl. Mater. Inter.*, 2011, **3**, 705-709.

11 Q. Zhou, Z. B. Zhao, Z. Y. Wang, Y. F. Dong, X. Z. Wang, Y. Gogotsi and J. S. Qiu, *Nanoscale*, 2014, **6**, 2286-2291.

12 S. M. Hao, Q. J. Li, J. Qu, F. An, Y. J. Zhang and Z. Z. Yu, *ACS Appl. Mater. Inter.*, 2018, **10**, 17923-17932.

13 S. J. Hao, B. W. Zhang, Y. Wang, C. J. Li, J. Y. Feng, S. Ball, M. Srinivasan, J. S. Wu, and Y. Z. Huang, *Electrochim. Acta*, 2018, **260**, 965-973.

14 B. B. Wang, X. Zhang, X. J. Liu, G. Wang, H. Wang and J. T. Bai, *J. Colloid. Interf. Sci.*, 2018, **528**, 225-236.

15 G. X. Gao, S. Y. Lu, B. T. Dong, Z. C. Zhang, Y. S. Zheng and S. J. Ding, *J. Mater. Chem. A*, 2015, **3**, 4716-4721.

16 Q. H. Wu, R. F. Zhao, X. Zhang, W. L. Li, R. H. Xu, G. W. Diao and M. Chen, *J. Power Sources*, 2017, **359**, 7-16.

17 X. L. Wang, Y. G. Liu, H. Arandiyan, H. P. Yang, L. Bai, J. Mujtaba, Q. G. Wang, S. H. Liu and H. Y. Sun, *Appl. Surf. Sci.* 2016, **389**, 240–246.